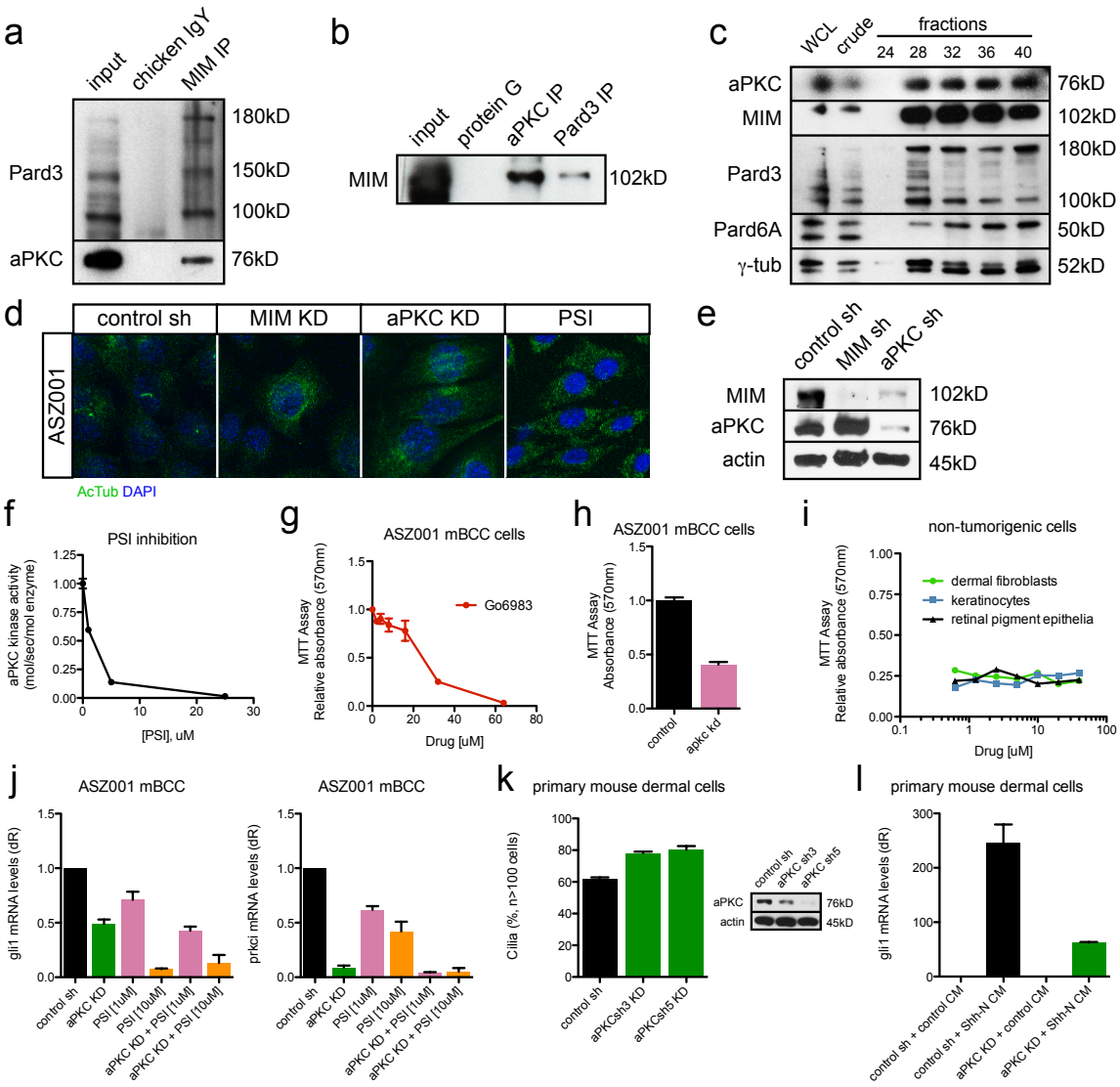


**Supplementary Figure 1: aPKC alters BCC cell growth. a, b,** Reciprocol immunoprecipitation of MIM-aPKC-Pard3 complexes from mouse dermal cells. **c,** Cofractionation of purified centrosome fractions from mouse fibroblasts. WCL, whole cell lysate. Crude, unpurified centrosome lysate. γ-tub, γ-tubulin. **d,** Cilia (Actub) after shRNA knockdown of MIM, aPKC, or inhibition of aPKC in BCC cells (n=3). sh, short-hairpin. KD, knockdown. **e** aPKC or MIM protein levels compared to actin. **f,** PSI suppresses *in vitro* aPKC activity (n=3). **g,** Pan PKC inhibitor Go6983 suppresses BCC cell growth (n=3). **h,** aPKC knockdown reduces BCC cell growth (n=3). **i,** PSI does not alter cell proliferation of mouse dermal fibroblasts, mouse keratinocytes, and human retinal pigment epithelial cells (n=3). **j,** aPKC inhibition and shRNA knockdown do not amplify loss of Hh signaling (n=3). **k, l,** Hh signaling and ciliogenesis are separable in mouse dermal cells after aPKC shRNA (n=3). Error bars, s.e.m.

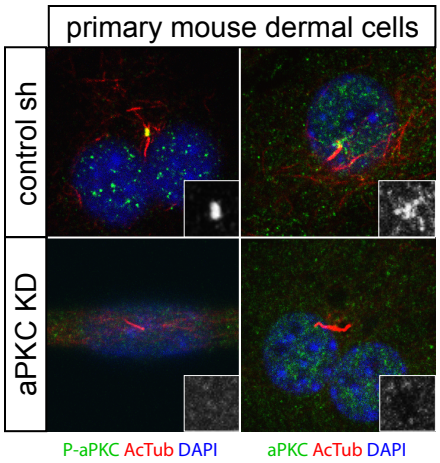


**Supplementary Figure 2: aPKC localizes to the basal body.** aPKC or P-aPKC found at the basal body of primary mouse dermal cells and immunoreactivity is reduced upon aPKC knockdown. Actub, acetylated tubulin.

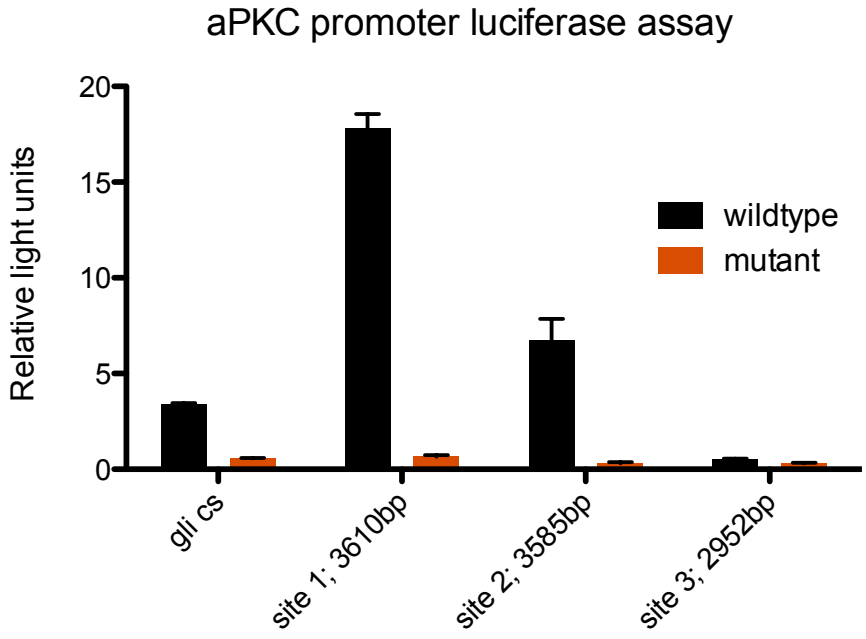


**Supplementary Figure 3: Functional Gli binding sites are found in the aPKC promoter.** Luciferase assay of multimerized Gli binding sites or their mutants show two functional Gli binding sites within the aPKC promoter (n=4). Gli cs, consensus sequence. Error bars, s.e.m.

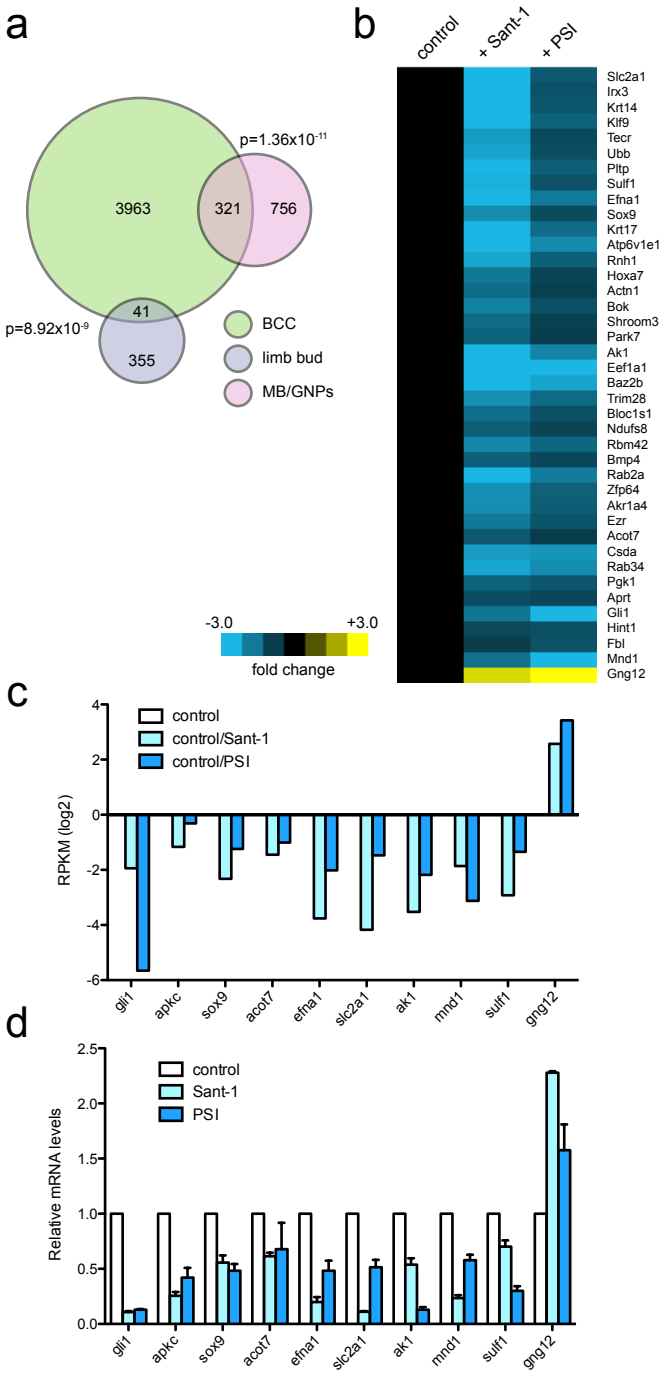


**Supplementary Figure 4: aPKC inhibition affects Hh target genes. a,** Venn diagram and **(b)** heatmap of commonly altered transcripts in both Sant-1 and PSI-treated samples compared to ChIP-Seq data sets from limb bud and medulloblastoma/GNPs. **c,** RPKM values and **(d)** subsequent validated transcript levels of commonly altered transcripts (n=3). Error bars, s.e.m.

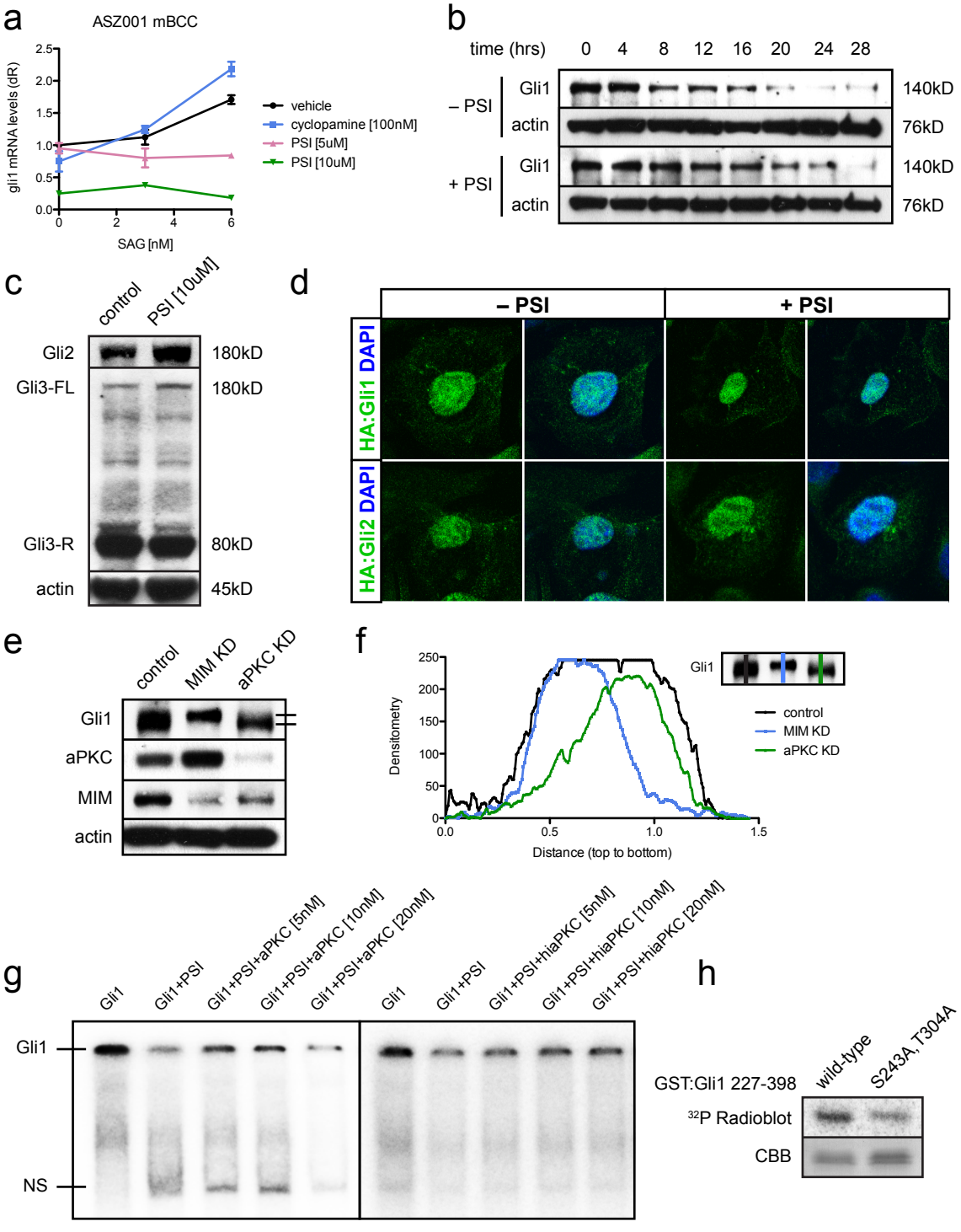


**Supplementary Figure 5: aPKC does not significantly affect Gli protein stability or processing. a,** SAG does not rescue reduced Hh signaling from PSI-treated BCC cells (n=3). Error bars, s.e.m. **b,** PSI modestly stabilizes Gli1 protein levels in BCC cells. **c,** Gli processing is not altered with PSI treatment in primary mouse dermal cells where no

loss of cilia is observed. **d,** PSI does not alter transfected nuclear HA:Gli protein localization in BCC cells. **e,** Gli1 protein has altered electrophoretic mobility with knockdown of aPKC or MIM. **f,** Densitometry graph of Gli1 protein. **g,** Over phosphorylation of IVT human Gli1 by aPKC disrupts DNA binding whereas heat-inactivated aPKC does not rescue DNA-binding of PSI-treated Gli1. **h,** GST:Gli1 227-398$^{S243A,T304A}$ accumulates less phosphorylation than wild-type protein when exposed to aPKC in an *in vitro* kinase assay.

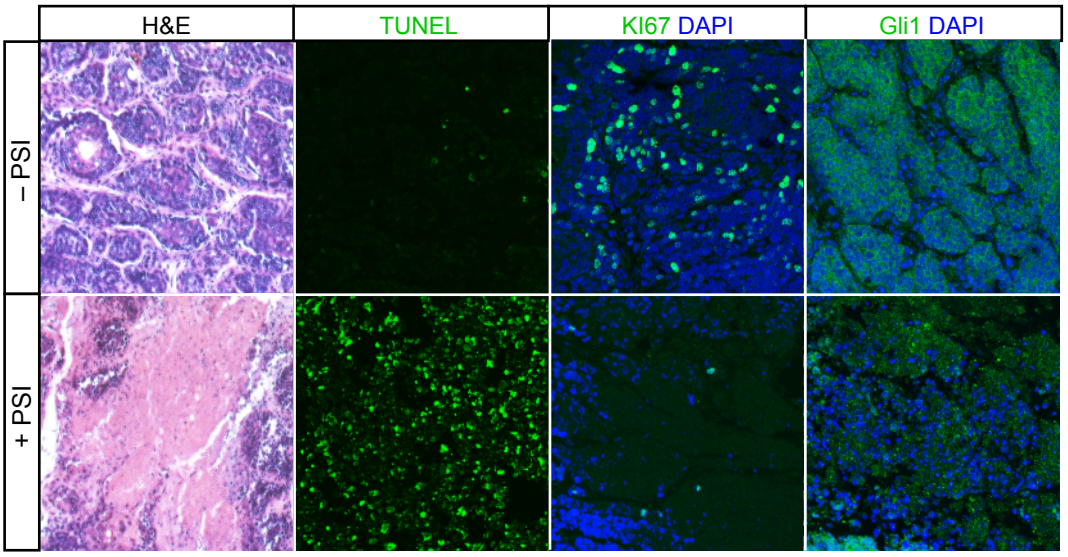


**Supplementary Figure 6: PSI disrupts tumor growth.** BCC tumors lose classical palisades, with an increase in TUNEL-positive cells and a decrease in KI67-positive cells and Gli1 stain.

| Value | DMSO | ± SEM | PSI | ± SEM |
|---|---|---|---|---|
| **Glucose** | 257.9 | 28.05 | 255 | 38.19 |
| **AST** | 277.9 | 73.7 | 233.6 | 134.6 |
| **ALT** | 227.8 | 80.55 | 148.4 | 99.95 |
| **AlkPhos** | 270 | 42.17 | 247.8 | 17.46 |
| **GGT** | 0 | 0 | 0.714 | 0.63 |
| **Bilirubin** | 0 | 0 | 0.015 | 0.012 |
| **Chol** | 108.3 | 7.473 | 105.2 | 8.271 |
| **BUN** | 20.38 | 1.281 | 22.22 | 1.597 |
| **Creat** | 0.463 | 0.042 | 0.489 | 0.031 |
| **Ca** | 11.16 | 0.295 | 11.41 | 0.316 |
| **Phos** | 11.88 | 0.63 | 12.01 | 0.641 |
| **T.P.** | 5.5 | 0.138 | 5.689 | 0.247 |
| **Albumin** | 3.175 | 0.098 | 3.256 | 0.108 |
| **Globulin** | 2.325 | 0.088 | 2.433 | 0.17 |
| **Na** | 152.4 | 0.754 | 151 | 0.926 |
| **K** | 8.05 | 0.573 | 8.2 | 0.851 |
| **Cl** | 109.8 | 0.701 | 110.1 | 0.811 |
| **Co2** | 24.3 | 1.521 | 26.8 | 1.536 |
| **WBC** | 6.991 | 0.833 | 9.422 | 0.858 |
| **RBC** | 8.745 | 0.266 | 8.916 | 0.243 |
| **HGB** | 13.92 | 0.239 | 14.41 | 0.337 |
| **HCT** | 44.3 | 0.828 | 46.18 | 1.228 |
| **MCV** | 50.78 | 0.727 | 51.81 | 0.665 |
| **MCH** | 15.98 | 0.23 | 16.2 | 0.247 |
| **MCHC** | 31.45 | 0.192 | 31.26 | 0.297 |
| **Platelet** | Adeq | Adeq | Adeq | Adeq |
| **Neutrophil** | 14.75 | 4.858 | 17.22 | 3.09 |
| **Lymphocyte** | 77.25 | 5.195 | 72.89 | 2.988 |
| **Monocyte** | 6.125 | 1.156 | 9 | 1.067 |

**Supplementary Figure 7: Topical PSI does not alter chemical or hematological parameters.** Topical treatment of mice with DMSO (n=8) or 0.8mg/kg PSI dissolved in DMSO (n=9) results in no significant differences in blood parameters. Error bars, s.e.m.

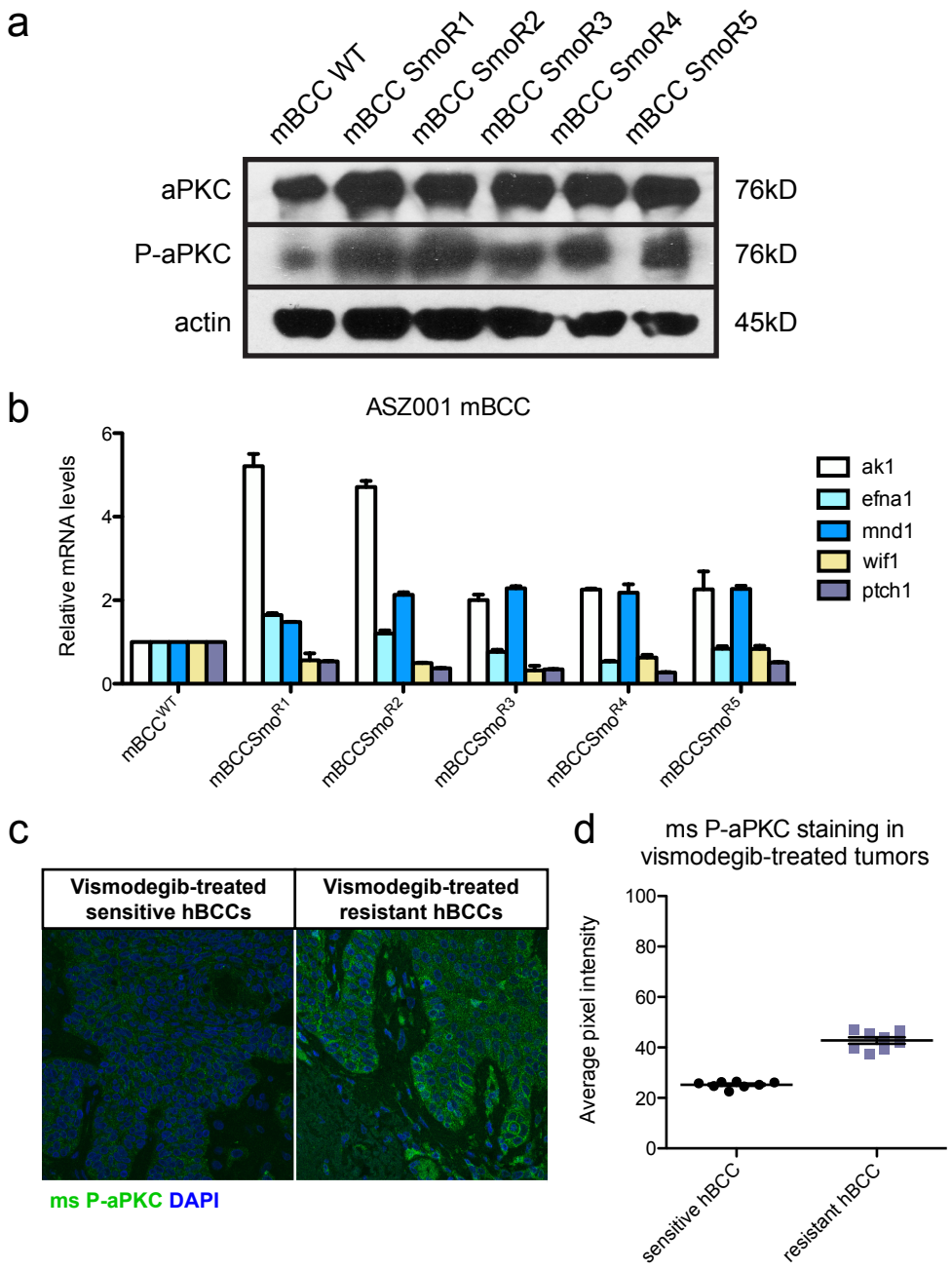


**Supplementary Figure 8: Vismodegib-resistant BCCs are positive for P-aPKC. a,** Total and activated aPKC protein levels are enriched in Smo antagonist-resistant cell lines. **b,** Gli target gene transcript levels are differentially regulated in Smo-resistant BCC cells and follow *gli1* mRNA levels, *apkc* levels, or are generally suppressed (n=3). **c,** Activated P-aPKC is enriched in vismodegib-treated resistant human BCCs (n=2) compared to vismodegib-sensitive tumors (n=2) using a mouse monoclonal antibody. **d,** Average pixel intensity of mouse monoclonal P-aPKC antibody stains in vismodegib-treated human tumors. Error bars, s.e.m.

| ChIP | forward oligo | reverse oligo | source |
|---|---|---|---|
| nanog | GGAAGAACCACTCCTACCAATACTCA | GTGTTTAAATTAATGTAGAGGCCTTCTG | Po et al, 2010 |
| ptch1-1 | ACAAAAGGAACGGAAAGTGT | AGCACGTTCCTCCAGTTTAC | Vokes et al, 2007 |
| ptch1-2 | CCAGGCTCTCTCTAACAAGC | ACAACATTATCGCTGGGAAT | Vokes et al, 2007 |
| rab34 | CAAAAGCTCCATTCTCACAA | AGGAAACTGGGAGAACATCA | Vokes et al, 2007 |
| nkx2-9 | CTACCAAGCGTGCCTAAAGT | TTTATCCCAGGGAGCTAAAG | Vokes et al, 2007 |
| hhip1 | TAAAAGGGCACACTTGAAAA | AATTGCTGCAGACCCTAAAT | Vokes et al, 2007 |
| actin | AGAAGGACTCCTATGTGGGTGA | ACTGACCTGGGTCATCTTTTC | Vokes et al, 2007 |
| gapdh | ACAACTTTGGCATTGAGGAA | GATGCAGGGATGATGTTCTG | IDT oligos |
| prkci-p1 | TTGGTCCTGAGAGGCTGAAG | GTTGGACAGCGATCATTGC | |
| prkci-p2 | GGCTGCGAAGATGGCTCTCC | GTACCACTTCCTTGAATTGG | |
| | | | |
| **qRTPCR** | | | |
| prkci | AAGGAACGATTGGGTTGTCACCCT | AAGGGTGGAACCACCTGCTTTTGCT | IDT oligos |
| prkcz | ACATCATCACGGACAACCCTGACA | TGTGAGGCCTTGACAGACAGGAAA | IDT oligos |
| cdc42 | GCAGGGCAAGAGGATTATGAC | TCTCAGGCACCCACTTTTC | IDT oligos |
| sulf1 | TGCTGAACAGTCACCCTGATCCAA | ACCACATGACTTGGGTCTTCACCT | IDT oligos |
| mnd1 | ATGACGGTATGGTTGACTGCGAGA | CCGGCCAACTCTTGCTTTCTCAAT | IDT oligos |
| efna1 | GTTTAACCAGCCCAACTGTGCCAT | AGGTCCGCACAGCTTGTTTCTTTG | IDT oligos |
| acot7 | TGTGTATTTACGGCAGGAGCAGGA | AATGTCTCCGTTCCTCCACTTGGT | IDT oligos |
| pard6a | CTGGGCTTCTACATTCGAGA | TGACAGTGACGATGAGGTTG | Realtimeprimers |
| sox9 | CCAGCGTTTAACCTTCAAGA | TGACCATACCCTTTGAGGAA | Realtimeprimers |
| slc2a1 | TGCCAAGCTAATCTGTAGGG | GAATGGGCGAATCCTAAAAT | Realtimeprimers |
| ak1 | GGAGTGTGAGCTGCCATAGA | GGGAAGTCACTAGGGATGGA | Realtimeprimers |
| gng12 | CTAAGCACCGGCAAATTAAA | GGTGGTTAGTGCCCATAGTG | Realtimeprimers |

**Supplementary Table 1.**